Engineering Geology 268 (2020) 105512

Contents lists available at ScienceDirect

Engineering Geology

journal homepage: www.elsevier.com/locate/enggeo

Region specific seismic hazard analysis of Krishna Raja Sagara Dam, India

P. Anbazhagan*, G. Silas Abraham

Department of Civil Engineering, Indian Institute of Science, Bangalore 560012, India

ARTICLE INFO

Keywords:
Maximum magnitude
DSHA
Probable earthquake locations
Peak ground acceleration
Peninsular India

ABSTRACT

Region-specific seismic hazard analysis was carried out for Krishna Raja Sagara Dam site in Karnataka, India. Seismic event data and seismic source data within a 500 km radius were collected. Deterministic seismic hazard analysis was conducted for different methods of earthquake magnitude and location estimation. It was observed that the ground motion estimates vary widely with different methods of M_{max} estimation and that the rupture based method, which calculates M_{max} based on fault dimensions, can give a reliable estimate of the possible maximum magnitude in regions of low to moderate seismicity. Based on this study, the greatest median ground motion at the dam site is estimated as 0.43 g and the ground motion required to be tolerated without catastrophic failure is considered as 0.11 g. In Stable Continental Regions across the world, where earthquake data is scarce, the methodology followed here can be adopted to conduct region-specific seismic hazard analysis.

1. Introduction

Peninsular India (PI), the southern part in particular, which is one of the oldest landmasses of the earth's crust, being an intraplate region was considered inert to younger earth movements and the related seismic activity (Ramasamy, 2006). However, recent seismic history shows that more than five damaging earthquakes with magnitudes greater than M_w 6.0 have occurred in PI, highlighting the importance of Seismic Hazard (SH) assessment (Jaiswal and Sinha, 2007). The most notable historical earthquakes of central and southern part of PI are Koyna (1967; M_w 6.3), Coimbatore (1900; M_w 6.3), Latur (1993; M_w 6.1) and Bellary (1843; M_w 5.9).

Failure of dams due to earthquakes is widely reported; in particular, several dams failed in the Stable Continent Region (SCR) during Bhuj 2001 Earthquake. Though it may not always cause a catastrophic failure, an earthquake can render a dam non-functional which can affect the socio-economic aspects of the region. Therefore, proper assessment of risk due to the impact of seismic activity on the dam should be evaluated to mitigate future losses. This risk assessment requires evaluation of SH at the dam site. SH can be evaluated in deterministic as well as probabilistic procedures. However, for critical structures, where failure is intolerable, deterministic procedures of hazard analysis are recommended (Krinitzsky, 1995). In this study, SH at a dam site in a SCR is evaluated considering regional parameters and is compared with conventional procedures to bring out the importance of regional specific approach in SH assessment.

Several SH studies were conducted in the recent past in PI. Sitharam and Anbazhagan (2007) conducted SH analysis of the Bangalore region; Jaiswal and Sinha (2007) estimated the SH of PI with a zoneless approach; Sitharam et al. (2012) carried out SH analysis for the entire Karnataka state; Anbazhagan et al. (2014) carried out SH analysis for Coimbatore city using a rupture based method. Most of the studies estimate SH for an entire state or for the whole region and only a few studies assess the region-specific SH in PI.

Seyrek and Tosun (2011) conducted SH studies on 36 dam sites in Turkey with dam heights ranging from 15 to 195 m. Seismic sources within a radius of 100 km were considered and Deterministic Seismic Hazard Analysis (DSHA) was performed using multiple attenuation relations. In low to moderate seismicity regions, peak ground acceleration (PGA) of the range 0.09–0.2 g was estimated and PGA up to 0.45 g was estimated in the near-source zones. Vetter et al. (1997) evaluated SH for three dam sites in Northcentral Colorado. Two methods of hazard analysis, Probabilistic Epicentral Distances (PED) method and Probabilistic Seismic Hazard Analysis (PSHA) were used. Pailoplee (2014) evaluated SH for 19 proposed dam sites along the Mekong river (South-East Asia). Earthquake records within 300 km from the sites were considered. Both DSHA and PSHA were done and ground shaking levels up to 0.44 g were estimated in deterministic analysis.

For region-specific hazard analysis of dams, International Commission on Large Dams (ICOLD) recommends consideration of information on tectonic and geologic setting in a radius of 100 km around the dam site which can be extended to 300 km to include major faults, and the region-specific attenuation characteristics along with the

* Corresponding author.
E-mail address: anbazhagan@iisc.ac.in (P. Anbazhagan).

https://doi.org/10.1016/j.enggeo.2020.105512
Received 9 April 2019; Received in revised form 17 January 2020; Accepted 30 January 2020
Available online 07 February 2020
0013-7952/

seismic history within a minimum radius of 100 km (ICOLD, 2009). According to Indian practice, the country is divided into zones depending on the past seismic activity, lithology, and tectonics. Each zone is assigned a zonal factor which corresponds to the PGA expected at that location based on the past seismic intensities. The present study area falls under Zone-II of Indian Seismic zonation which corresponds to a PGA of 0.1 g (IS 1893 (Part 1), 2016). However, this zonation does not consider regional geology and seismicity (Anbazhagan, 2013). Very limited systematic region-specific hazard analysis was carried out for Indian Dams. In this study, region-specific SH analysis of Krishna Raja Sagara (KRS) dam was carried out as part of Dam Rehabilitation and Improvement Programme (DRIP) using deterministic procedures. The results are compared with previous studies in the region and the Indian seismic code to suggest a suitable method for SH assessment of critical structures in regions with scarce seismic data.

2. Study area

KRS Dam is a gravity dam in the Mandya region of Karnataka, India. It has a total catchment area of 10,619 sq. km. The dam is 39.8 m high, 2620 m long with a reservoir capacity of 1368.85 million cubic meters. This dam falls under the category of *Large Dam* according to ICOLD specifications. The stored water in the reservoir is used for irrigation purposes in the state of Karnataka and Tamil Nadu and the water discharged from this dam is stored in Mettur dam in Salem district of Tamil Nadu, India.

The area around the study site where information related to seismotectonic features are utilized to estimate seismic hazard at the site is termed as Seismic Study Area (SSA) (Anbazhagan et al., 2014). Federal Emergency Management Agency (FEMA, 2005) guidelines suggest SSA of radial extent of 100 km around the site for a dam. In this study, the extent of SSA is chosen based on the past regional damage distribution due to seismic activity. Coimbatore earthquake (M_w 6.3; 1900), which is the most damaging earthquake in the region had an influence distance (MKS Intensity IV) up to 480 km. Therefore, it was decided that SSA of 500 km radial extent should be able to capture the seismicity of the region.

Comprehensive knowledge and information about the geological setting and active faults, major and minor lineaments in the SSA are required for SH analysis. The major tectonic constituents in PI include the massive Deccan Volcanic Province (DVP), Southern Granulite Terrain (SGT), Dharwar Craton (DC), Cuddapah Basin (CB), Godavari Graben (GG) and Eastern and Western Ghats on the coastal regions. The geology of the study area is shown in Fig. 1. Major part of the SSA falls under DC and SGT. DC has higher strain rates than other SCRs, is seismically active and has hosted some of the deadliest earthquakes in the past (Rao, 2015). It was observed that the region including the study area, Mandya should be segregated under Zone-III rather than Zone-I (currently Zone-II) of the Indian standard code due to moderate seismic activity in these regions (Ganesha Raj and Nijagunappa, 2004). The soil of Mandya district is derived from granites and gneisses interpreted with occasional patches of schist. However, the dam is constructed on granites and gneisses hard rock formation.

3. Seismotectonics of the Dam site

The dam SSA is part of PI, which is grouped under SCRs. The seismic activity in this region is mostly due to reverse faulting aligned roughly normal to the azimuth of convergence between the Indian and Eurasian plates (Vita-finzi, 2004). Several authors have mapped the faults and weak zones in PI where earthquakes can occur. The tectonic features of the study area were collected from the Seismotectonic Atlas (SEISAT) published by Geological Survey of India (SEISAT, 2000) and from published literature: Ramasamy (2006), Balakrishnan et al. (2009), Gupta (2006), Kayal (2008) and Rao (2000). The fault information gathered in the SSA of KRS dam is shown in Fig. 2.

The earthquake event information was gathered from several sources such as Indian Meteorological Department (IMD), International Seismological Centre (ISC), United State Geological Survey (USGS), European Mediterranean Seismological Centre (EMSC), Oldham (1883), Kayal (2008) and Rao (2015). The event data was homogenized to moment magnitude (M_w) using conversion equations provided by Nath et al. (2017) and was declustered using the time and space window algorithm proposed by Gardner and Knopoff (1974). The earthquake data in the region overlaid on the map is shown in Fig. 3. The cumulative number of events starting from 1900 CE is given in Fig. 4 (a). The profile is stepped with a negligible number of events in the magnitude range, M_w 4–4.6. This can be due to insufficient data, change in earthquake detectability over time or it can be the earthquake characteristic of the region. Also, each earthquake is assumed to have occurred on the fault which is closest to the epicentre of the event. This is a reasonable assumption for the regions where surface evidence of faulting is not available and where epicentres of most of the earthquakes are located close to the assigned seismic sources. In this study region, around 94% of the earthquake epicentres are within 10 km of some source.

Magnitude of completeness, M_c estimation is critical for hazard assessment studies and was computed using the Goodness of Fit Test

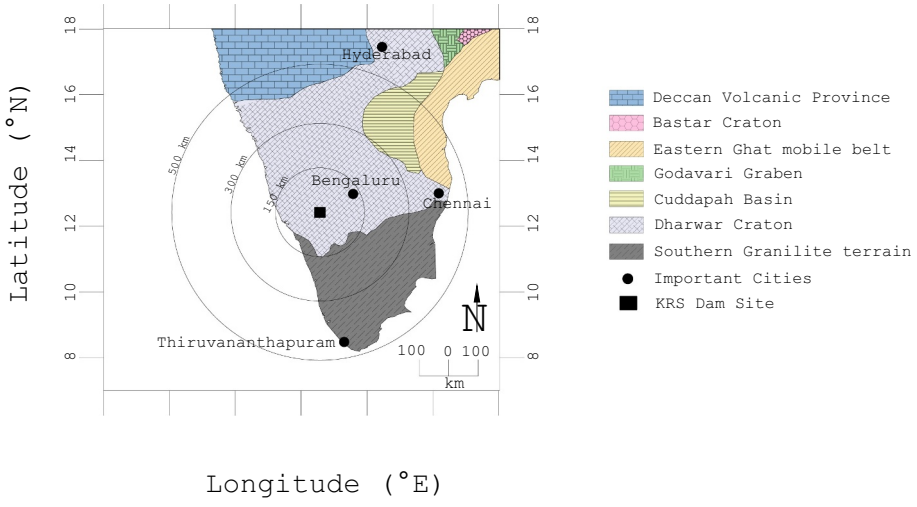

Fig. 1. Geology of the Study area around KRS dam site.

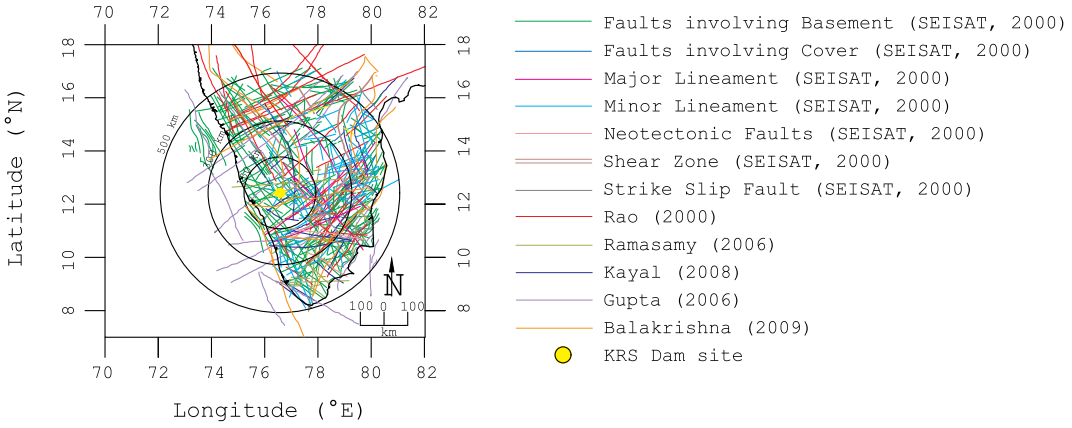

Fig. 2. Seismic Sources in the Study area.

(GFT) proposed by Weimer and Wyss (2000). M_c was computed for different time intervals with spacing of 10 years starting from 1900 CE The magnitude of completeness was found to be M_w 4.6 for the past 118 years (1900–2018) and M_w 3.3 for the past 28 years (1990–2018). The spatial variation of M_c was not considered in this study. Though the shorter 28-year catalogue is complete over a wider magnitude range, it does not represent the long-term seismicity of the region. As earthquakes of magnitude, $M_w > 4$ are of engineering interest, the frequency magnitude relation was derived based on the longer period sample (1900–2018), which is complete for $M_w > 4.6$. Seismic parameters '*a*' and '*b*' of the Gutenberg-Richter relationship, ($\log \lambda = a - b M_w$) were computed for regions of different radial extent (150 km, 300 km, 500 km) from the dam site using least-squares regression. The frequency magnitude relations and the associated plots are shown in Fig. 4 (b-d). The '*b*' value for this region increases with increase in the radial extent of SSA and the estimated values of '*b*' are 0.95, 1.14, 1.27 for 150 km, 300 km, 500 km respectively. This is due to the decrease in the proportion of higher magnitude earthquakes ($M_w > 5.5$) with an increasing radius of SSA. This can be attributed to the larger areas enclosing more of the relatively quiescent SGT than the 150 km SSA. As '*b*' values are used to infer seismicity of the region, it gives varying results of SH when different SSAs are considered.

4. Maximum magnitude estimation

In a deterministic analysis, maximum earthquake, M_{max} is defined as the Maximum Credible Earthquake (MCE) which is based on a reasonable assessment of maximum earthquake potential in the current tectonic setting (Reiter, 1990). Proper assessment of this is crucial for SH analysis and there are several methods for its estimation both deterministic and statistical in nature. In regions of high seismic activity where the historical record encompasses the total earthquake potential of the region, M_{max} can be taken equal to the maximum earthquake magnitude observed in the past, (M_{max}-*obs*). For regions of low and moderate activity, several methods are available for estimation of M_{max} based on Magnitude increment, Seismicity rate, Magnitude-Frequency extrapolation of historical record, Saturation of body wave magnitude, m_b (Wheeler, 2009). Statistical procedures for M_{max} estimation were provided by Kijko and Singh (2011) and some of these can be applied when no information about the nature of the earthquake magnitude distribution is available and when the earthquake catalogue is incomplete. Most of the above-mentioned methods for M_{max} estimation give varying values of M_{max} based on the extent of SSA, which in turn affects the hazard value at the site. However, rupture based method is based on the regional rupture character of the region gives the same

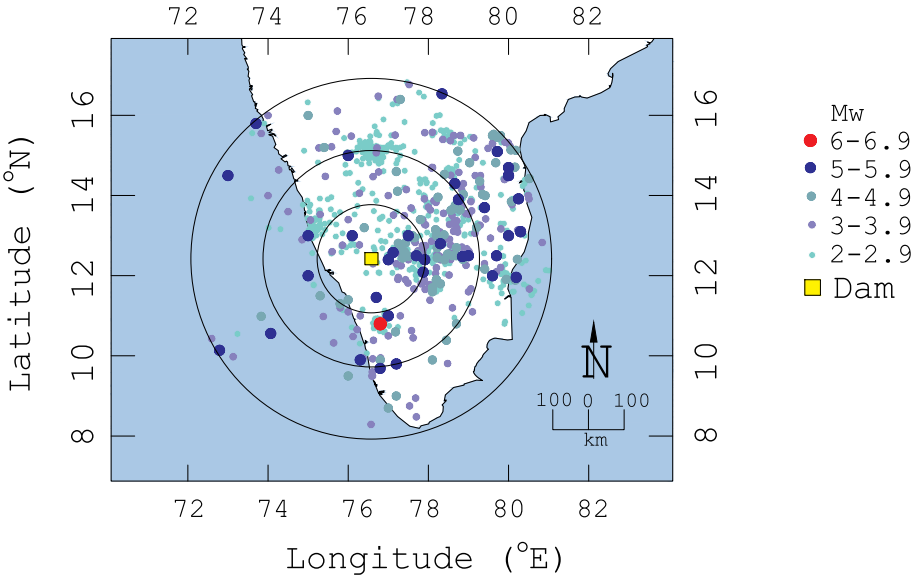

Fig. 3. Past Seismicity of the Study area.

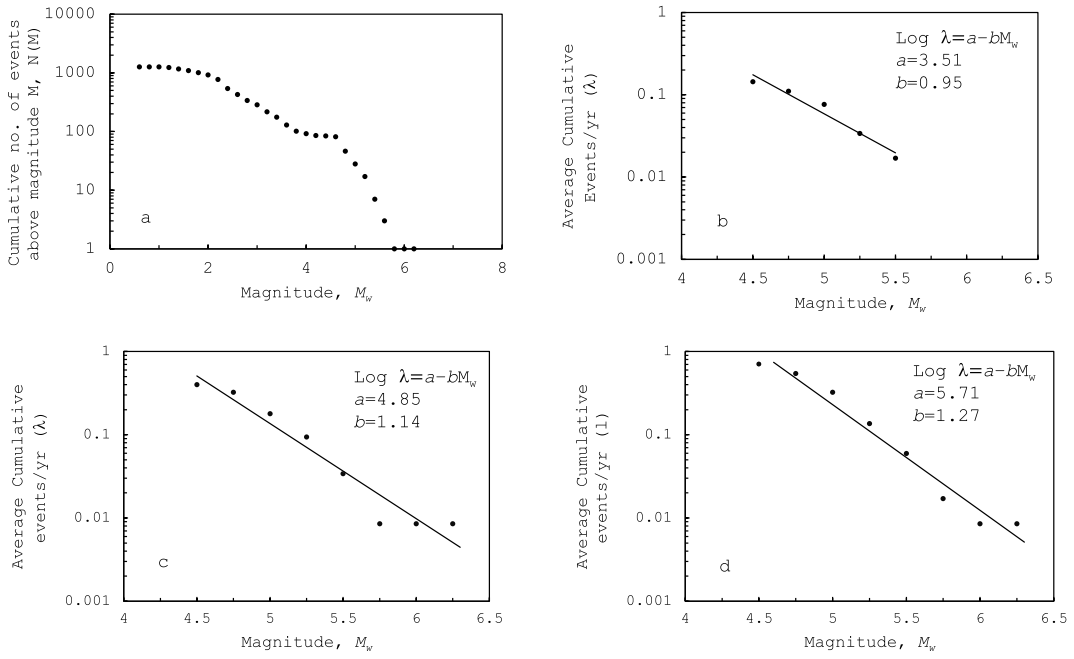

Fig. 4. (a) Cumulative number of events from 1900 CE, Gutenberg-Richter relationship for Seismic Study area of (b) 150 km, (c) 300 km, (d) 500 km radial extent from KRS dam site.

value of M_{max} even for different extent of SSA (Anbazhagan et al., 2015). In the present study, SH analysis was conducted using M_{max} estimated using different methods.

4.1. Conventional procedures

The maximum observed historic earthquake on each fault gives the lower bound of the maximum earthquake that can possibly occur on that source. It is possible that an unrecorded event of higher magnitude might have occurred on that fault outside the duration of the available catalogue. Therefore, maximum observed magnitude is incremented, which is the equivalent of increasing the duration of the available earthquake catalogue for regions where recurrence interval of the maximum magnitude event is longer than the duration of the available earthquake record (Budnitz et al., 1997; Wheeler, 2009). In this study, a 0.5 magnitude unit increment, which is the equivalent of increasing the duration of the catalogue by a factor of 2.8–3.2 for regions with '*b*' value in the range of 0.9–1.0, was considered. Another approach is that, as maximum historic earthquake indicates the maximum earthquake potential of a region, an earthquake of the maximum observed magnitude can be expected to occur on any of the sources in the region. In the absence of data on seismic activity of individual faults, a very conservative estimate can be made by assuming that each of the sources is capable of producing such high magnitude earthquake and consequently the maximum possible earthquake on each source can be taken as this maximum magnitude. As in the case above, to compensate for the short duration of the earthquake catalogue, Tate-Pisarenko estimator of M_{max} (TP), which is a statistical parametric estimator that predicts an increment to the observed maximum magnitude in the region based on the Gutenberg-Richter frequency magnitude distribution of earthquake, was used. For this study, the statistical increment was estimated using the '*a*' and '*b*' parameters from 150 km SSA. Use of increments based on *b* value from 300 km and 500 km gives very high magnitudes ($M_w > 8$) which is unreasonably high for the earthquake potential for SCRs as the maximum instrument recorded earthquake in SCR is Bhuj, 2001 (M_w 7.6) and the maximum historic earthquake in SCRs is New Madrid Earthquake (1811–1812, M_w 7.5) and even the geological records in this region of pre-1811 events indicate maximum magnitudes in the range 7–8 (USGS). Under the conventional procedures of M_{max} estimation, the following four cases were considered.

- Magnitude is equal to the maximum magnitude observed on each fault (C1)
- Magnitude is equal to maximum magnitude observed on each fault incremented by 0.5 magnitude units (C2) i.e. if a maximum observed earthquake on a fault is M_w 5, the maximum earthquake magnitude possible on that source in the future is taken as M_w 5.5
- Magnitude on all the faults is equal to the maximum magnitude observed in the region (M_w 6.3 for all the faults in this case) (C3)
- Magnitude on all the faults is equal to the maximum magnitude observed in the region incremented by the value obtained from statistical estimate (C4)

Here, C1 and C2 consider only the faults in the region which have past earthquakes assigned to them, whereas C3 and C4 consider all the faults in the region irrespective of the previous earthquake on the fault.

4.2. Rupture based method

As earthquake magnitude is well correlated with rupture dimensions, if rupture dimensions associated with maximum historical earthquake on a fault are estimated, the maximum magnitude possible on other faults in that tectonic setting can be assessed by fault dimension-magnitude correlations (Budnitz et al., 1997). As the percent fault rupture (PFR) (Subsurface ruptured length/Length of the fault) is well correlated with the maximum earthquake magnitude and is a representative of the rupture character of the region (Anbazhagan et al., 2014), it can be used to estimate the magnitude. The earthquakes of magnitude $M_w > 5$ were selected assuming that they have sufficiently ruptured the source and PFR vs Length of the fault for each of the corresponding sources was plotted for different radial extents of SSA. The subsurface ruptured length of the faults was calculated using the relation given by Wells and coppersmith (Wells and Coppersmith, 1994). The PFR of the fault decreases as the fault length increases and it follows a similar trend irrespective of the extent of SSA as shown in Fig. 5. The rupture character is slightly different for 150 km radius SSA

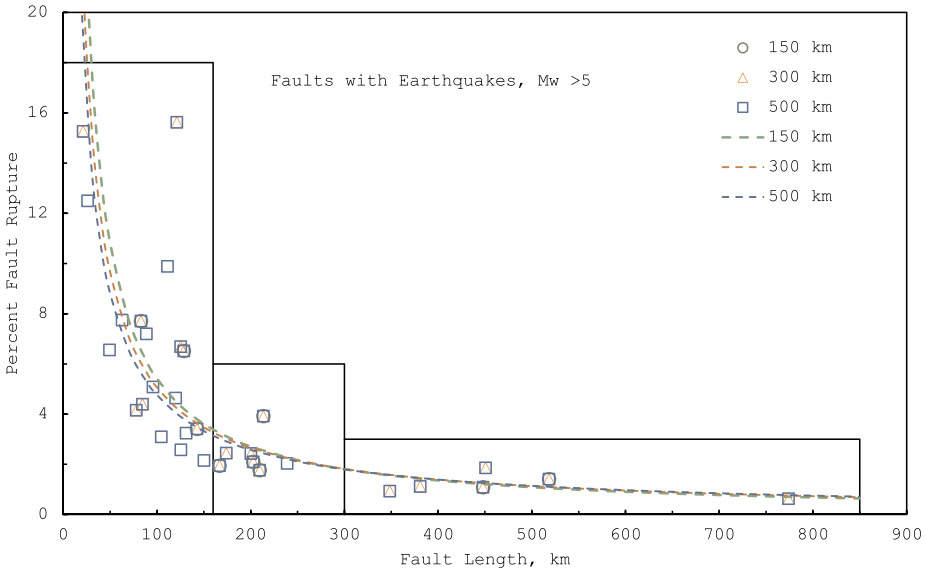

Fig. 5. Regional Rupture Character of KRS dam site.

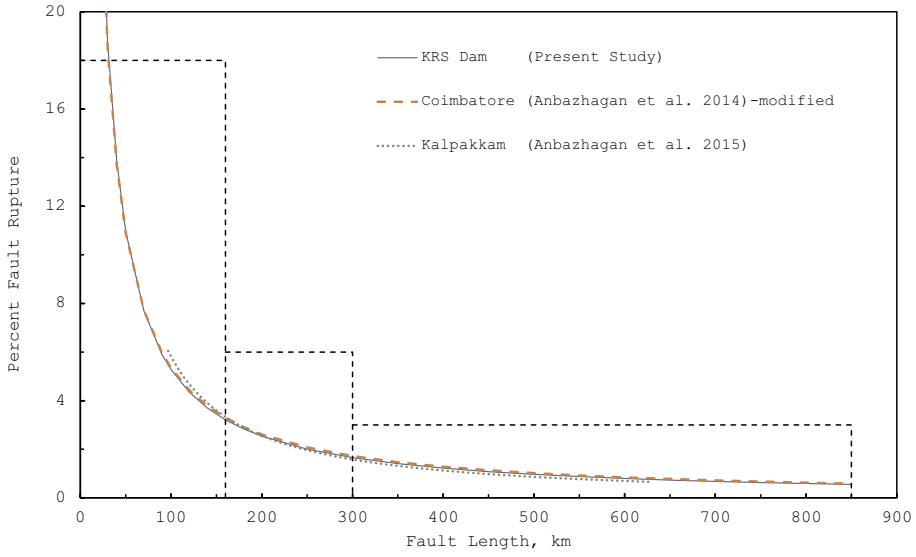

Fig. 6. Comparison of Regional Rupture Character of KRS dam site, Coimbatore and. Kalpakkam.

as most of it lies in DC whereas for 300 km and 500 km SSA, provinces of DC and SGT are enclosed, and it results in an averaged rupture character which is similar for both the extents. The rupture character of KRS dam site is comparable with the rupture character of Kalpakkam (Anbazhagan et al., 2015) and Coimbatore region (Anbazhagan et al., 2014). Fig. 6 shows a comparison of the regional rupture character of Kalpakkam, Coimbatore and KRS dam site. A modified version of the Coimbatore rupture character is presented in Fig. 6 which was estimated using an updated source map and is slightly different from Anbazhagan et al. (2014). This difference is only for the fault length less than 200 km and it does not affect the maximum rupture percent and magnitude estimation. As the 500 km SSAs of KRS dam and Coimbatore overlap to a major extent, the rupture character is similar for both the regions whereas a slight difference has been observed with the rupture character of Kalpakkam region. Based on the established rupture character (Fig. 5), the faults were divided into categories based on their length, 20 km–160 km, 160 km–300 km and 300 km–850 km and a value enveloping the maximum PFR was assigned to each category, 18%, 6%, and 3% respectively and the maximum magnitude (C5) on each fault was back-calculated from the subsurface rupture length. The maximum percent rupture was so chosen to encompass the previous rupture fractions to give a maximum subsurface rupture length and thereby a maximum magnitude.

5. Estimation of ground motion

The ground motion at a site due to a distant earthquake can be estimated using Ground Motion Prediction Equations (GMPEs). However, number of GMPEs developed for the study area/PI are limited and the ground motion attenuation of PI is similar to Eastern North America (ENA) (Iyengar and Raghu Kanth, 2004). So, GMPEs developed for ENA region can be used to predict ground motions in PI.

To determine the efficacy of a GMPE to predict ground motions in a target region, several assessment methods were proposed (Azarbakht et al., 2014). Of them, the quantitative assessment of the GMPEs proposed by Scherbaum et al. (2009) is based on the Kullback–Leibler (KL)

Table 1
Ground Motion Prediction Equations (GMPEs) considered for seismic hazard analysis.

S. No.	GMPE	Abbreviation
	Peninsular India GMPE	
1	Iyengar and Raghu Kanth (2004)-Southern India	RAIY[SI]-04
2	NDMA (2010)	NDMA-10
3	Bajaj and Anbazhagan (2019)-Variable Stress drop	KAPA-VS19
4	Bajaj and Anbazhagan (2019)-Constant Stress drop	KAPA-CS19
	Similar Region GMPE (ENA)	
5	Hwang and Huo (1997)	HAHO-97
6	Toro et al. (1997)	TOR-97
7	Atkinson and Boore (2006), modified in Atkinson and Boore (2011)	ATBO-06-11
8	Campbell (2003)	CAM-03
9	Tavakoli and Pezeshk (2005)	TAPE-2005
10	Pezeshk et al. (2011)	PEZA-11
11	Boore and Atkinson (2008), modified in Atkinson and Boore (2011)	BA-08-11

distance between the unknown original model, f and the candidate model, g (GMPE) which is selected for a particular tectonic setting. For a discrete case and for comparison between the candidate models, Log-Likelihood (LLH) of the model g can be calculated as given by the equation below.

$$LLH := -\frac{1}{N}\sum_{i=1}^{N} log_2(g(x_i)) \quad (1)$$

where x_i, $i = 1, 2, \ldots, N$ denote the observations.

A lower value of LLH indicates that the candidate model, g is close to the model that has generated the data, f, while a higher value of LLH indicates that it is highly improbable that the observations can be explained by model g. The value of LLH can be used to rank the models based on their ability to estimate the observed ground motions. This method has also an advantage of using macroseismic intensity data instead of strong-motion data where the latter is scarce.

In this study, a total of 11 GMPEs were selected for the whole region, 4 developed for PI and 7 developed for ENA, and were ranked using the above mentioned LLH method. The list of GMPEs considered for this study are provided in Table 1. The LLH method was applied using the macroseismic intensity data of the past earthquakes within the SSA. The intensity data for the earthquakes was taken from the electronic supplement of Martin and Szeliga (2010) and the Intensity to PGA conversion was done by the relation developed for the Indian Subcontinent by Nath and Thingbaijam (2011). The intensity, intensity data locations and the corresponding PGA values for each earthquake are provided in Table 2. As several of the selected GMPEs are applicable only for $M_w > 5$ and few other GMPEs are not applicable for near field ground motions, the GMPEs were ranked according to the radial distances of 0 km–50 km, 50 km–200 km, 200 km–500 km from the respective epicentres and for magnitudes $M_w > 5$ and $M_w < 5$ separately. Bellary (1843), Coimbatore (1900), Kerala (1953), Mysore (1970) and Pondicherry (2001) earthquakes were considered for $M_w > 5$ and Shimoga (1975), Bangalore (1984), Idukki (2000), Idukki (2001) and Bangalore (2001) earthquakes were considered for $M_w < 5$. The details of each earthquake, the intensity data points, and the estimated PGA are provided in the Appendix. As the location estimate for historic earthquakes is approximate, the earthquakes were assumed to have occurred at the respective hypocentres and various distance measures required for different GMPEs were calculated with this assumption. Also, the site conditions where the intensity data is available play a crucial role in amplification and thereby in the estimation of bedrock PGA at the site. In most parts of PI, the thickness of soil deposits is too low to produce a considerable amplification of the ground motions; therefore, the PGA estimated at the surface can be approximated to the PGA at bedrock. Nevertheless, both the cases of no amplification and amplification due to presence of National Earthquake Hazards Reduction Program (NEHRP) D-class site for all the intensity stations as per Sitharam et al. (2015), were evaluated to estimate the dependence of site class on GMPE selection and on the final estimated PGA at the dam site. For site amplification, factors from Boore and Joyner (1997) were used. The final LLH value was calculated as a weighted mean of the LLH calculated from individual earthquakes. Further, Data Support Index (DSI), which indicates how much the available data support or reject the model in comparison with the state of uninformativeness (Delavaud et al., 2012) was calculated for each of the model GMPE and weights were assigned to the GMPEs based on their DSI.

For the purpose of calculation of DSI, the weight of each GMPE is calculated using their Weighted Mean LLH values in Eq. (2).

$$w_i = \frac{2^{-LLH(g_i)}}{\sum_{k=1}^{n} 2^{-LLH(g_k)}} \quad (2)$$

n is the number of GMPEs applicable to that magnitude and distance range.

$$DSI = 100\frac{w_i - w_{uni}}{w_{uni}} \quad (3)$$

w_i refers to the weight of each GMPE, w_{uni} is the weight of each GMPE if every model has the same contribution ($w_{uni} = 1/n$).

Further, the LLH values of only the GMPEs which have positive DSI are used to calculate the final weights using Eq. (2).

Tables 2 and 3 list the GMPEs used to predict the ground motion at different radial distances, their corresponding LLH values and the weight of each GMPE for $M_w > 5$ and $M_w < 5$ respectively with no assumption of amplification at the intensity data locations and Tables 4 and 5 gives the list of GMPEs assuming site class-D for all the intensity data locations. The ground motion due to an earthquake was evaluated as a weighted mean of ground motion from each GMPE and wherever discontinuity was observed in the distance from the epicentre (100 km and 300 km), the PGA values were interpolated. For the epicentral distance range of 300–500 km and for $M_w < 5$, no intensity data points were available and therefore, the same GMPEs selected for 100–300 km epicentral distance range and for $M_w < 5$ were used. Being present in SCR, this area has neither high rates of seismicity nor nearby high slip rate faults, therefore only median PGA value was considered. Another reason for considering the median PGA is that the rupture character of the region is selected encompassing all the previous percent rupture values and thereby is expected to give a conservative estimate of maximum magnitude. The standard deviation values of the estimated PGA are provided to aid in realizing the uncertainty. The median PGA values obtained for different magnitudes for different hypocentral distances are shown in Fig. 7.

6. Deterministic seismic hazard analysis

A maximum earthquake magnitude was selected for each source and

Table 2
Log-likelihood Values, Data Support Index and Ranking for $M_w > 5$ (No Amplification at intensity locations).

Earthquake	Kerala (1953)	Mysore (1970)	Pondicherry (2001)	Bellary (1843)	Coimbatore (1900)		
GMPE	*LLH*	*LLH*	*LLH*	*LLH*	*LLH*	*M.LLH*	DSI (wt)
Dist. Range				**0 km–100 km**			
CAM-03	7.78 (2)	7.00 (6)	3.70 (3)	20.50 (1)	2.70 (12)	5.05	112.64 **(0.21)**
TOR-97	7.30 (2)	6.50 (6)	3.00 (3)	10.30 (1)	2.20 (12)	4.12	307.29 **(0.40)**
HAHO-97	34.10 (2)	31.80 (6)	16.30 (3)	67.60 (1)	6.50 (12)	18.90	−99.99 (0.00)
ATBO-06-11	19.80 (2)	15.50 (6)	3.60 (3)	62.70 (1)	7.730 (12)	12.45	−98.74 (0.00)
KAPA-VS19	8.30 (2)	7.50 (6)	4.70 (3)	20.40 (1)	2.30 (12)	5.17	96.77 **(0.19)**
KAPA-CS19	19.50 (2)	17.20 (6)	8.90 (3)	43.12 (1)	3.50 (12)	10.56	−95.32 (0.00)
BA-08-11	8.80 (2)	8.10 (6)	5.20 (3)	23.50 (1)	4.20 (12)	6.47	−20.54 (0.00)
RAIY[SI]-04	37.90 (2)	37.10 (6)	21.88 (3)	72.00 (1)	9.40 (12)	22.87	−100 (0.00)
TAPE-05	6.80 (2)	6.10 (6)	3.30 (3)	25.80 (1)	3.20 (12)	5.17	96.75 **(0.19)**
PEZA-11	30.50 (2)	23.74 (6)	6.60 (3)	86.80 (1)	10.60 (12)	18.20	−99.98 (0.00)
NDMA-10	20.60 (2)	19.30 (6)	10.90 (3)	49.70 (1)	5.30 (12)	12.63	−98.88 (0.00)
Dist. Range				**100 km–300 km**			
CAM-03	3.23 (3)	NA	8.86 (5)	11.20 (8)	9.08 (15)	9.02	−72.41 (0.00)
TOR-97	2.18 (3)	NA	5.46 (5)	6.20 (8)	4.38 (15)	4.81	411.58 **(0.55)**
HAHO-97	10.93 (2)	NA	19.71 (3)	15.15 (6)	21.52 (6)	17.71	−99.93 (0.00)
ATBO-06-11	6.27 (3)	NA	27.27 (5)	34.37 (8)	22.00 (15)	24.52	−100 (0.00)
KAPA-VS19	1.42 (3)	NA	5.06 (5)	6.59 (8)	5.06 (15)	5.10	317.01 **(0.45)**
KAPA-CS19	2.21 (3)	NA	11.41 (5)	14.89 (8)	10.00 (15)	10.74	−91.6 (0.00)
RAIY[SI]-04	13.70 (3)	NA	39.07 (5)	43.74 (8)	31.44 (15)	34.13	−100 (0.00)
TAPE-05	2.35 (3)	NA	8.94 (5)	13.11 (8)	11.71 (15)	10.72	−91.48 (0.00)
PEZA-11	10.75 (3)	NA	41.28 (5)	54.63 (8)	39.84 (15)	41.08	−100 (0.00)
NDMA-10	3.95 (3)	NA	18.45 (5)	23.99 (8)	18.32 (15)	18.42	−99.96 (0.00)
Dist. Range				**300 km–500 km**			
CAM-03	NA	NA	6.35 (2)	NA	9.66 (9)	9.06	−93.76 (0.00)
TOR-97	NA	NA	3.62 (2)	NA	4.28 (9)	4.16	86.09 **(0.34)**
ATBO-06-11	NA	NA	15.35 (2)	NA	22.86 (9)	21.49	−100 (0.00)
KAPA-VS19	NA	NA	1.79 (2)	NA	3.55 (9)	3.23	254.69 **(0.66)**
KAPA-CS19	NA	NA	3.77 (2)	NA	7.58 (9)	6.89	−71.97 (0.00)
TAPE-05	NA	NA	5.97 (2)	NA	12.19 (9)	11.06	−98.44 (0.00)
PEZA-11	NA	NA	26.50 (2)	NA	43.26 (9)	40.21	−100 (0.00)
NDMA-10	NA	NA	11.02 (2)	NA	18.13 (9)	16.84	−99.97 (0.00)

The number in the parentheses in the LLH column denotes the number of intensity points used in arriving at the LLH value. M.LLH denotes the Weighted mean LLH for each GMPE. The weight of each GMPE is given in parentheses along with DSI values. The GMPEs which have a positive DSI and which were assigned weightage are given in bold.

PGA at the dam site due to an earthquake of magnitude M_{max} on each source at a closest distance to the site was calculated. Two minor lineaments (SEISAT, 2000) pass below the dam section and the earthquakes in the vicinity of these structures are in the range M_w 2.2–4.7 with the lowest magnitude and highest magnitude events occurring at 45 km and 130 km from the dam site. As the ground displacement plays a major role in case of event on these faults and as most of the GMPEs give a reasonable estimate of ground motion beyond 1 km, the above

Table 3
Log-likelihood Values, Data Support Index and Ranking for $M_w < 5$ (No Amplification at intensity locations).

Earthquake	Bangalore (2001)	Idukki (2001)	Bangalore (1984)	Idukki (2000)	Shimoga (1975)		
GMPE	*LLH*	*LLH*	*LLH*	*LLH*	*LLH*	*M.LLH*	DSI (wt)
Dist. Range				**0 km–100 km**			
ATBO-06-11	9.07 (15)	9.68 (10)	2.79 (11)	5.44 (10)	6.56 (5)	6.88	−80.77 (0.00)
KAPA-VS19	3.59 (15)	1.49 (10)	1.98 (11)	2.32 (10)	2.68 (5)	2.49	301.54 **(1.00)**
KAPA-CS19	11.35 (15)	2.04 (10)	4.6 (11)	5.29 (10)	6.05 (5)	6.36	−72.46 (0.00)
RAIY[SI]-04	21.57 (15)	5.19 (10)	5.43 (11)	13.32 (10)	13.49 (5)	12.47	−99.6 (0.00)
NDMA-10	9.62 (15)	2.44 (10)	2.95 (11)	4.95 (10)	5.60 (5)	5.46	−48.71 (0.00)
Dist. Range				**100 km–300 km**			
ATBO-06-11	3.25 (2)	6.81 (9)	5.53 (1)	3.51 (9)	4.12 (8)	4.75	−65.07 (0.00)
KAPA-VS19	1.65 (2)	2.3 (9)	1.61 (1)	1.31 (9)	1.95 (8)	1.83	165.44 **(0.69)**
KAPA-CS19	4.01 (2)	3.72 (9)	3.8 (1)	2.13 (9)	2.87 (8)	3.01	16.52 **(0.31)**
RAIY[PI]-04	20.09 (2)	10.79 (9)	18.19 (1)	12.40 (9)	8.78 (8)	11.63	−99.7 (0.00)
NDMA-10	4.57 (2)	4.51 (9)	4.48 (1)	2.71 (9)	2.89 (8)	3.51	−17.19 (0.00)

The GMPEs which have a positive DSI and which were assigned weightage are given in bold.

Table 4
Log-likelihood Values, Data Support Index and Ranking for $M_w > 5$ (Amplification corresponding to site class D at intensity locations).

Earthquake	Kerala (1953)	Mysore (1970)	Pondicherry (2001)	Bellary (1843)	Coimbatore (1900)		
GMPE	*LLH*	*LLH*	*LLH*	*LLH*	*LLH*	*M.LLH*	DSI (wt)
Dist. Range				**0 km–100 km**			
CAM-03	13.19 (2)	12.52 (6)	8.63 (3)	37.81 (1)	5.36 (12)	9.56	408.58 **(0.53)**
TOR-97	16.87 (2)	15.31 (6)	8.74 (3)	17.77 (1)	5.37 (12)	9.75	346.32 **(0.47)**
HAHO-97	81.60 (2)	76.13 (6)	51.82 (3)	130.12 (1)	22.93 (12)	49.20	−100 (0.00)
ATBO-06-11	59.46 (2)	49.73 (6)	26.57 (3)	125.5 (1)	13.25 (12)	32.56	−100 (0.00)
KAPA-VS19	18.45 (2)	16.90 (6)	12.58 (3)	35.58 (1)	6.22 (12)	11.93	−1.25 (0.00)
KAPA-CS19	45.35 (2)	40.60 (6)	27.96 (3)	79.10 (1)	11.24 (12)	26.34	−100 (0.00)
BA-08-11	21.66 (2)	19.89 (6)	15.57 (3)	43.17 (1)	12.13 (12)	16.59	−96.1 (0.00)
RAIY[SI]-04	86.46 (2)	83.96 (6)	60.70 (3)	135.05 (1)	31.62 (12)	57.22	−100 (0.00)
TAPE-05	16.59 (2)	15.26 (6)	11.23 (3)	46.78 (1)	9.19 (12)	13.14	−57.56 (0.00)
PEZA-11	83.25 (2)	70.06 (6)	39.69 (3)	173.99 (1)	24.16 (12)	48.74	−100 (0.00)
NDMA-10	50.31 (2)	46.89 (6)	33.99 (3)	92.32 (1)	18.25 (12)	33.14	−100 (0.00)
Dist. Range				**100 km–300 km**			
CAM-03	4.92 (3)	NA	5.98 (5)	4.21 (8)	4.21 (15)	4.57	975.58 **(1.00)**
TOR-97	7.61 (3)	NA	12.39 (5)	12.44 (8)	9.74 (15)	10.66	−84.22 (0.00)
HAHO-97	42.36 (2)	NA	52.59 (3)	42.58 (6)	59.70 (6)	50.36	−100 (0.00)
ATBO-06-11	31.05 (3)	NA	67.11 (5)	73.82 (8)	55.82 (15)	59.89	−100 (0.00)
KAPA-VS19	4.98 (3)	NA	12.56 (5)	14.14 (8)	11.27 (15)	11.61	−91.86 (0.00)
KAPA-CS19	12.34 (3)	NA	30.40 (5)	33.53 (8)	25.01 (15)	26.85	−100 (0.00)
RAIY[SI]-04	45.45 (3)	NA	84.88 (5)	88.00 (8)	70.86 (15)	75.09	−100 (0.00)
TAPE-05	8.07 (3)	NA	19.98 (5)	26.30 (8)	26.23 (15)	23.48	−100 (0.00)
PEZA-11	45.38 (3)	NA	97.00 (5)	113.93 (8)	96.48 (15)	96.13	−100 (0.00)
NDMA-10	19.05 (3)	NA	44.28 (5)	50.12 (8)	42.73 (15)	42.59	−100 (0.00)
Dist. Range				**300 km–500 km**			
CAM-03	NA	NA	7.42 (2)	NA	4.44 (9)	4.98	582.07 **(1.00)**
TOR-97	NA	NA	9.89 (2)	NA	9.62 (9)	9.66	−73.5 (0.00)
ATBO-06-11	NA	NA	50.82 (2)	NA	57.72 (9)	56.46	−100 (0.00)
KAPA-VS19	NA	NA	6.58 (2)	NA	8.17 (9)	7.88	−8.59 (0.00)
KAPA-CS19	NA	NA	17.26 (2)	NA	20.15 (9)	19.63	−99.97 (0.00)
TAPE-05	NA	NA	15.99 (2)	NA	27.09 (9)	25.08	−100 (0.00)
PEZA-11	NA	NA	77.94 (2)	NA	102.65 (9)	98.15	−100 (0.00)
NDMA-10	NA	NA	33.85 (2)	NA	42.52 (9)	40.94	−100 (0.00)

The GMPEs which have a positive DSI and which were assigned weightage are given in bold.

two sources are excluded from the analysis. Further detailed site studies are required to estimate the ground motion due to these sources. The average focal depth of recent earthquakes in PI was 15 km which agrees with the depth range (10 km–15 km) for SCR regions (Kayal, 2008). For this study, a uniform focal depth of 15 km was considered for all the earthquakes. The estimated PGA values for the cases of '*No Amplification*' and '*Amplification corresponding to D-class site*' at the intensity data points, along with their standard deviations are provided for different methods of M_{max} selection in Table 6. For the rupture based method, the maximum magnitude was estimated considering the rupture capacity of the source depending on its dimensions. Also, in rupture based analysis, as the magnitude is linked to the fault dimensions, a

Table 5
Log-likelihood Values, Data Support Index and Ranking for $M_w < 5$ (Amplification corresponding to site class D at intensity locations).

Earthquake	Bangalore (2001)	Idukki (2001)	Bangalore (1984)	Idukki (2000)	Shimoga (1975)		
GMPE	*LLH*	*LLH*	*LLH*	*LLH*	*LLH*	*M.LLH*	DSI (wt)
Dist. Range				**0 km–100 km**			
ATBO-06-11	22.6 (15)	5.08 (10)	16.71 (11)	16.34 (10)	21.39 (5)	16.55	−99.40 (0.00)
KTVS-18	8.87 (15)	3.34 (10)	6.82 (11)	6.96 (10)	7.67 (5)	6.85	399.24 **(1.00)**
KTCS-18	28.97 (15)	8.98 (10)	18.67 (11)	18.8 (10)	20.05 (5)	19.96	−99.94 (0.00)
RAIY[SI]-04	55.82 (15)	20.55 (10)	28.57 (11)	42.53 (10)	43.92 (5)	39.25	−100.00 (0.00)
NDMA-10	27.3 (15)	8.32 (10)	16.59 (11)	19.37 (10)	20.9 (5)	19.09	−99.90 (0.00)
Dist. Range				**100 km–300 km**			
ATBO-06-11	23.41 (2)	17.68 (9)	32.22 (1)	24.16 (9)	17.28 (8)	20.48	−99.99 (0.00)
KTVS-18	4.6 (2)	3.5 (9)	6.53 (1)	4.34 (9)	3.58 (8)	3.96	395.48 **(1.00)**
KTCS-18	16.11 (2)	9.38 (9)	18.19 (1)	12.03 (9)	8.98 (8)	10.86	−95.85 (0.00)
RAIY[SI]-04	57.3 (2)	33.7 (9)	54.98 (1)	43.32 (9)	32.74 (8)	38.79	−100 (0.00)
NDMA-10	20.95 (2)	12.34 (9)	21.91 (1)	16.12 (9)	12.01 (8)	14.35	−99.63 (0.00)

The GMPEs which have a positive DSI and which were assigned weightage are given in bold.

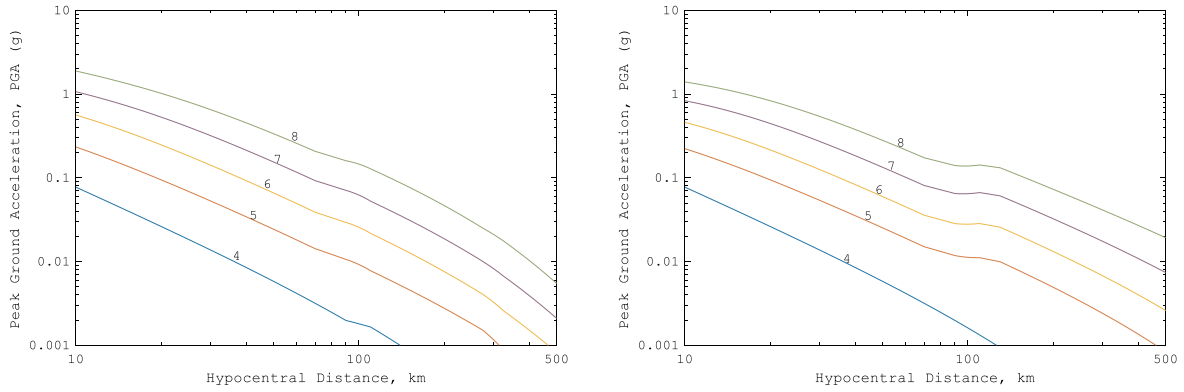

(a) Assuming no amplification at the intensity locations

(b) Assuming amplification of NEHRP D-class site at intensity locations

Fig. 7. Peak Ground Acceleration (PGA) at different Hypocentral distances for magnitudes. M_w (4–8).

Table 6
Peak ground acceleration (PGA) at the dam site with different methods of M_{max} estimation.

Method of M_{max} estimation	Critical event		PGA ($\sigma_{ln(PGA)}$)	
	Magnitude	Epicentral distance, km	No amplification at intensity locations	D-class site amplification at intensity locations
C1	5.5	23	0.11 (0.36)	0.10 (0.47)
C2	6	23	0.17 (0.36)	0.16 (0.46)
C3	6.3	6	0.52 (0.44)	0.47 (0.54)
C4	6.1	6	0.45 (0.44)	0.41 (0.55)
C5	6.4	11	0.43 (0.40)	0.39 (0.50)

No Amplification at intensity locations refers to the case where the intensity measurements used for the GMPE selection procedure are assumed to have occurred on at sites with no significant amplification and *Amplification corresponding to site class D at intensity locations* refers to the case where the intensity measurements are assumed to have occurred on a D-class site.
PGA stands for Peak Ground Acceleration and the value in the parenthesis is the standard deviation of ln(PGA).

proper weightage is given to all the faults depending on their length and thereby to their earthquake producing capacity. Though the rupture method gives a reliable estimate of M_{max} on each fault in the region, it has to be estimated whether the fault is yet to rupture or has already ruptured in the past or has no seismicity associated to it. If the fault is yet to rupture, the probable location of rupture on the fault should also be evaluated.

7. Probable future rupture zones

As an earthquake process is usually related to the release of accumulated strain energy, it is unlikely that a major earthquake will occur at the same location in the near future (100–200 years). Supporting this, there had been no major re-rupture of any seismogenic source in India for the past 500 years except for the eastern plate boundary (Martin and Szeliga, 2010). Also, it was assumed that the earthquakes of lower magnitude ($M_w < 5$) might not have ruptured the seismic source sufficiently to release all the accumulated strain energy and are therefore probable locations for future earthquakes with minor events in their vicinity being evidence for their seismic activity. So, a probable future rupture zone was selected according to the following criteria.

— The location must have experienced at least one minor ($M_w < 5$) earthquake in the past 20 years to indicate seismic activity
— There must be a defined seismic source within 10 km radius of the epicentre of the above-mentioned minor earthquake and the source should not have been assigned to any previous major earthquake ($M_w > 5$).
— The location should not fall in the rupture zone of any previous large magnitude earthquake ($M_w > 5$).

The rupture zone for a major earthquake was demarcated by a circular zone with its centre at the epicentre of the earthquake and its radius calculated from Wells and Coppersmith (Wells and Coppersmith, 1994) relation of subsurface rupture length estimation. For simplicity, the radius for all the rupture zones was taken as 12.7 km, the value corresponding to M_w 6 earthquake. Based on these criteria, 28 locations were identified as probable future rupture locations as shown in Fig. 8. The magnitude of earthquake possible at each of these locations was estimated using the rupture based method on the faults within a 10 km radius of that location. If two or more faults are within the specified radius, the maximum of the magnitudes on these faults was considered to be the magnitude at that location. The median PGA values at the site due to earthquakes at three locations within the 150 km SSA along with their standard deviation values are provided in Table 7.

8. Results and discussions

SH analysis was carried out for KRS dam using different methods of M_{max} estimation and PGA values at the site were estimated. The results vary widely depending on the method of M_{max} estimation. The median PGA values are slightly lower and the standard deviation values are higher when D-class site conditions are assumed at the intensity data locations. As mentioned previously, as amplification is not significant in PI, only the case of '*no amplification at intensity data locations*' is considered further. The PGA with M_{max}-*obs* (C1) is around 0.11 g and is

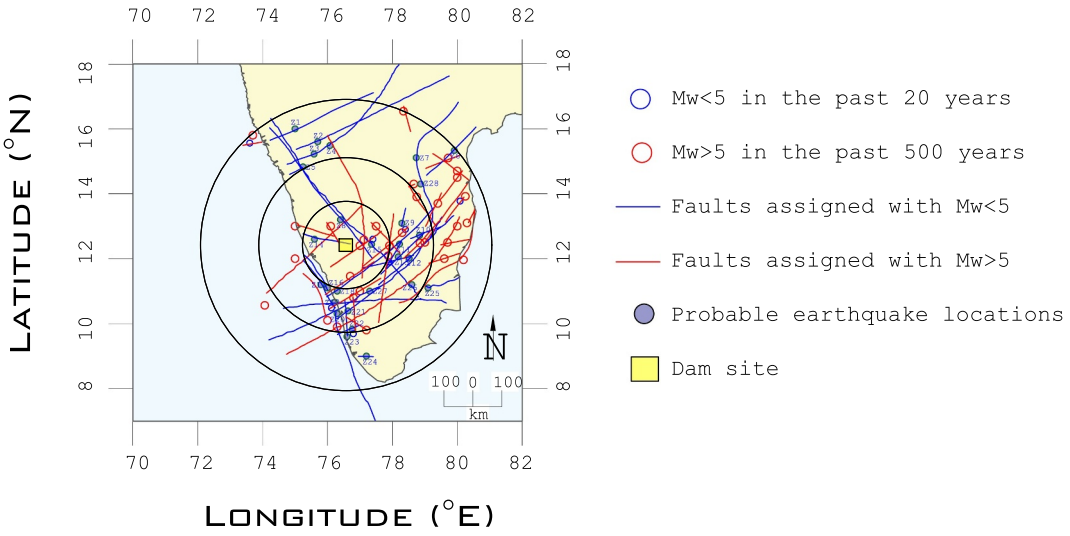

Fig. 8. Probable Earthquake Locations in the Study area.

Table 7
Peak ground acceleration (PGA) at the dam site with event at probable future rupture locations.

Zone	Magnitude	Epicentral distance, km	PGA ($\sigma_{ln(PGA)}$)	
			No amplification at intensity locations	D-class site amplification at intensity locations
Z15	6.5	87	0.05 (0.36)	0.05 (0.46)
Z8	6.2	88	0.04 (0.36)	0.03 (0.47)
Z14	5.8	110	0.02 (0.39)	0.02 (0.61)

No Amplification at intensity locations refers to the case where the intensity measurements used for the GMPE selection procedure are assumed to have occurred on at sites with no significant amplification and *Amplification corresponding to site class D at intensity locations* refers to the case where the intensity measurements are assumed to have occurred on a D-class site.
PGA stands for Peak Ground Acceleration and the value in the parenthesis is the standard deviation of ln(PGA).

approximately equal to the PGA 0.1 g recommended in the IS codes based on past seismicity. The 0.5 magnitude unit increment method (C2) gives a PGA of 0.17 g which is comparable with some of the previous SH studies for PI (0.165 g with return period of 2475 years, Sitharam et al., 2012; 0.15–0.30 g for 2475-year return period, Vipin et al., 2009). Also, there are some studies that give a PGA value lower than the one obtained above (0.08–0.1 g, Anbazhagan et al., 2014; 0.01–0.02 g, Parvez et al., 2017). The considerably lower value of Parvez et al. (2017) can be attributed to the consideration of earthquake activity only in specific seismogenic zones which are far from the present target site.

The PGA value estimated using the regional maximum earthquake on all the faults irrespective of their dimensions, (C3) is 0.52 g. The statistical method of increment to the regional maximum earthquake is dependent on the '*b*' value and gives varying increment values for varying SSA. The estimate from 150 km SSA gives an increment of 0.5 units; however, for 300 km and 500 km SSA, as the '*b*' values are high it gives an increment of 1.8 units which correspond to $M_w > 8$. This is due to the problem in scaling of seismic parameters in regions of low seismicity and therefore this method of M_{max} estimation should be used with caution if the seismic parameters change drastically with change in the extent of SSA. The PGA value obtained from increment (using 150 km SSA) of regional maximum magnitude (C4) is 0.45 g. This method assumes equal earthquake potential for all the faults irrespective of their dimensions which may not be plausible.

The PGA evaluated using rupture based method (C5) is 0.43 g. This method considers the length of the faults and the regional rupture character in obtaining the M_{max} and is, therefore, a more region-specific approach than the former ones. However, based on past seismicity, it is unlikely that a major earthquake will occur in the same region/fault in the next 50 years as the average return periods of damaging earthquakes are more than 300 years (Anbazhagan et al., 2014). Therefore, probable earthquake locations were identified where future rupture of fault can take place and the PGA at the dam site due to earthquakes at these locations is evaluated to be 0.05 g which matches closely with the PGA of 0.04 g with a return period of 2500 years recommended by NDMA (NDMA, 2010) for Bangalore region. From this study, it can be observed that the worst-case scenario median PGA in the region considering earthquake on all faults with rupture locations on each being closest to the dam site is 0.43 g; the expected PGA at the site due to earthquake at the locations where future rupture is expected is 0.05 g. FEMA (FEMA, 2005) guidelines recommend consideration of ground motion due to Maximum Credible Earthquake (MCE), which causes the greatest possible ground motion at the site and due to Maximum Design Earthquake (MDE), which the dam should be able to withstand with some tolerable damage yet without a catastrophic failure like uncontrolled discharge of reservoir. For regions of high seismicity or if failure of structure poses a high risk, MCE needs to be used for design. However, if it is of low hazard, a lower value can be used. In this case, the greatest possible PGA can be taken as 0.43 g from rupture based method, and the PGA which should be used for design or to be tolerated without a catastrophic failure can be based on the past seismicity of the region which is 0.11 g or can be taken as 0.05 g obtained from the consideration of probable future rupture zones which is also comparable with the value 0.04 g provided by NDMA, (2010). However, Indian Standard Code (IS 1893 (Part 1), 2016) recommends a minimum PGA of 0.1 g for design purposes of important structure if region-specific analysis result is less than the zone value. Therefore, PGA of 0.1 g can

be considered for tolerable damage. This value can be used for safety assessment and design of dam associated facilities useful for the next decade or until there is a change of probable seismic event locations. Though SH analyses of dams and tailing dams were conducted in the past, there is no region-specific hazard analysis considering regional rupture character. Methodology followed in this study can be a suitable approach to arrive at the region-specific greatest possible ground motions and ground motions required to be tolerated without catastrophic failure of a dam. Nevertheless, the above values are only at the bedrock level and further studies considering the stratigraphy of the ground are required to evaluate the effect of site conditions to ascertain the safety of the dam.

Gravity dams are known to perform well during earthquakes. Out of ten concrete gravity dams subjected to peak horizontal ground accelerations in excess of 0.3 g around the world, only one suffered a major damage (Nuss et al., 2012). It suggests that the damage to the dam due to a distant earthquake is not significant.

The limitations of the study include the following aspects. The site effects of ground shaking were not considered and only PGA at the bedrock has been evaluated in this study. The site effects should be assessed for complete SH analysis of the dam. However, as the dam is built on rock stratum, the modification of ground motion is expected to be negligible. Dams are critically affected by the surface displacements due to ground motion of the near faults. Of the two minor lineaments passing under the dam section, there has been no geological study conducted on their rupture characteristics. Therefore, a study considering the possible rupture of the faults in the immediate vicinity of the dam and their effect on the performance of the dam needs to be undertaken. This study does not consider the unavailable geological evidence of the return period of earthquakes on faults or any geological evidence to support the occurrence of specific magnitudes. So, SH of the dam site can be reviewed in the future if the above studies are carried out. Also, as the dam is in operation since 1938, the deterioration of the construction materials and their effect on the seismic performance of the dam should be evaluated.

9. Conclusions

Region-specific hazard analysis was conducted for the dam site using different methods of M_{max} estimation. The attenuation relations used for predicting the ground motions at the site were selected based on their statistical expectation of log-likelihood of observed ground motions. The method of selecting the expected maximum magnitude, M_{max} as the maximum observed magnitude on the fault assumes that the maximum earthquake on each fault has occurred in the duration of the available catalogue which may not be true for regions of low to moderate seismicity. The method of increment to maximum observed magnitude on each fault has the drawback that the increment value is subjective. Assigning maximum regional magnitude to all the faults overestimates or underestimates the earthquake potential on the faults. The statistical method of determining the increment value to the regional maximum magnitude on all the faults is dependent upon the seismic parameters and gives widely varying values if seismicity parameters differ largely with the extent of seismic study area. Therefore, this method should be used with caution in such cases. Rupture based method, which is dependent on the rupture character of the faults in a given region and the source dimensions gives an estimate of maximum magnitude on the faults independent of the extent of study area. Using this method, the estimated PGA at the site is 0.43 g. Based on the analysis, PGA of 0.43 g may be considered as the greatest possible median ground motion due to Maximum Credible Earthquake and 0.1 g may be considered as the ground motion required to be tolerated without catastrophic failure of the dam.

Declaration of Competing Interest

The authors declare that they have no known competing financial interests or personal relationships that could have appeared to influence the work reported in this paper.

Acknowledgement

The authors would like to thank the Dam Safety (Rehabilitation) Directorate, Central Water Commission for funding the project entitled “Capacity Buildings in Dam Safety” under Dam Rehabilitation and Improvement Project” Ref: 07/1/2010/DSRD dated 08/12/2016.

Appendix. List of earthquakes used for GMPE selection

Unless mentioned otherwise, all the Epicentres and Magnitudes were taken from Amateur Seismic Centre (ASC), http://www.asc-india.org/ ,Pune, India (last accessed on 9th August 2019) and the magnitude conversion was done using equations from Nath et al., 2017.), http://www.asc-india.org; last accessed on 9th August 2019) and the magnitude conversion was done using equations from Nath et al. (2017).

Coimbatore Earthquake – 08-02-1900

Epicentre: 10.8 N, 76.8 E

Magnitude: ~ 6.3 (Basu, 1964) (M_L converted to M_w using the graphical relation of Heaton et al., 1986)

Depth of focus: ~ 60 km (Basu, 1964)

Lat.	Long.	Intensity EMS 98	*ED, km	PGA (g)
11.01	76.97	6	30	0.131
11.33	76.7	7	60	0.297
11.35	76.79	6	61	0.114
11.38	76.73	7	65	0.290
11.4	76.69	6	68	0.110
11.09	77.35	5	68	0.043
11.42	76.87	7	69	0.284
11.42	76.67	7	70	0.283
11.43	76.88	5	71	0.042
11.09	77.49	4	82	0.015
10.23	77.49	5	99	0.037
11.27	77.58	5	100	0.037
9.95	76.33	4	108	0.014
11.34	77.73	4	118	0.013
11.25	75.78	4	122	0.013
11.68	77.76	4	143	0.012

12.31	76.64	5	169	0.029
9.91	78.12	3	175	0.004
10.86	78.69	2	207	0.002
10.8	78.7	2	208	0.002
9.15	77.99	4	225	0.010
8.71	77.44	3	243	0.004
12.97	77.59	5	256	0.024
12.75	78.34	5	274	0.023
12.94	78.26	6	286	0.057
11.52	79.32	4	286	0.009
13.14	78.13	4	298	0.008
12.51	79.12	4	316	0.008
11.77	79.55	5	319	0.021
11.4	79.69	2	322	0.001
10.79	79.84	2	332	0.001
12.67	79.28	4	341	0.008
13.34	74.75	2	360	0.001
13.21	79.11	2	367	0.001
12.85	79.7	4	389	0.007
13.08	80.27	4	455	0.007
6.92	79.85	4	546	0.006
18.9	72.82	2	997	0.001

Lat. and Long. are the coordinates of the Intensity location
ED stands for Epicentral distance
PGA stands for Peak Ground Acceleration at the location

Bellary Earthquake – 01-04-1843
Epicentre: 15.2 N, 76.9 E
Magnitude: ~ 5.9 (M_L converted to M_w using the graphical relation of Heaton et al., 1986)
Depth of focus: NA (Avg. depth of 15 km was assumed)

Lat.	Long.	Intensity EMS 98	ED, km	PGA (g)
15.14	76.92	4	7	0.042
16.16	76.52	5	114	0.037
15.82	78.04	4	140	0.013
14.51	75.8	3	141	0.005
16.51	76.76	5	146	0.033
16.57	76.82	6	153	0.082
16.5	77.52	3	159	0.005
12.96	77.59	1	260	0.001
17.38	78.48	1	295	0.0005

Lat. and Long. are the coordinates of the Intensity location
ED stands for Epicentral distance
PGA stands for Peak Ground Acceleration at the location

Pondicherry Earthquake – 26-09-2001
Epicentre: 11.984 N, 80.225 E
Magnitude: ~ 5.5
Depth of focus: ~ 10 km

Lat.	Long.	Intensity EMS 98	ED, km	PGA (g)
11.94	79.83	5	43	0.063
11.76	79.76	4	56	0.021
12.7	79.97	4	84	0.017
12.84	79.7	4	111	0.015
13.09	80.26	5	123	0.036
13.22	79.1	2	184	0.002
13.63	79.41	2	203	0.002
13.14	78.13	2	261	0.001
12.97	77.58	3	307	0.003
13.3	77.53	2	327	0.001
12.88	74.84	2	593	0.001

Lat. and Long. are the coordinates of the Intensity location
ED stands for Epicentral distance
PGA stands for Peak Ground Acceleration at the location

Shimoga Earthquake – 12-05-1975
Epicentre: 1 0.8 N, 76.8 E
Magnitude: ~ 4.8
Depth of focus: NA (Avg. depth of 15 km was assumed)

Lat.	Long.	Intensity EMS 98	ED, km	PGA (g)
13.68	75.24	4	15	0.037
14.33	74.89	5	74	0.047
13.34	74.75	4	78	0.018
14.04	76.17	3	98	0.006
14.46	75.92	4	99	0.016
12.87	74.84	4	115	0.014
13.31	76.24	3	115	0.006
14.9	75.4	4	123	0.014
13.63	76.68	4	150	0.012
15.35	75.14	3	173	0.004
15.45	75	3	186	0.004
15.45	76.69	5	237	0.025
12.97	77.59	3	264	0.003

Lat. and Long. are the coordinates of the Intensity location
ED stands for Epicentral distance
PGA stands for Peak Ground Acceleration at the location

Idukki Earthquake – 12-12-2000
Epicentre: 9.824 N, 76.763 E
Magnitude: ~ 4.7
Depth of focus: ~ 10 km

Lat.	Long.	Intensity EMS 98	ED, km	PGA (g)
9.85	76.96	4	22	0.035
9.59	76.52	5	37	0.069
10.01	76.3	5	55	0.056
9.49	76.32	5	61	0.053
9.26	76.78	5	63	0.052
10.37	76.99	3	66	0.008
10.58	76.93	3	86	0.007
10.65	77.01	3	96	0.006
10.51	76.21	4	97	0.016
10.58	77.24	3	99	0.006
8.95	77.31	3	114	0.006
11	76.96	3	133	0.005
9.58	77.95	3	133	0.005
11.27	76.62	3	162	0.005
11.35	76.79	3	170	0.004
11.41	76.69	3	177	0.004
11.42	76.88	3	178	0.004
11.45	77.43	3	195	0.004
11.45	75.68	4	216	0.010

Lat. and Long. are the coordinates of the Intensity location
ED stands for Epicentral distance
PGA stands for Peak Ground Acceleration at the location

Idukki Earthquake – 07-01–2001
Epicentre: 9.801 N, 76.548 E
Magnitude: ~ 4.6
Depth of focus: ~ 25.4 km

Lat.	Long.	Intensity EMS 98	ED, km	PGA (g)
9.71	76.69	6	19	0.199
9.59	76.52	5	24	0.073
9.66	76.76	6	28	0.180
9.59	76.7	6	29	0.178
9.76	76.84	5	32	0.066
9.85	76.97	5	47	0.057
9.97	77.05	5	58	0.052
9.26	76.78	5	65	0.049
9.6	77.2	3	75	0.007
10	77.36	3	92	0.006

10	77.48	3	104	0.006
8.96	77.13	5	113	0.037
11	76.97	3	141	0.005
8.82	77.38	6	142	0.085
8.5	76.95	3	151	0.005
9.58	77.96	3	157	0.005
8.72	77.69	3	174	0.004
11.25	75.78	3	182	0.004
8.8	78.15	3	208	0.004

Lat. and Long. are the coordinates of the Intensity location
ED stands for Epicentral distance
PGA stands for Peak Ground Acceleration at the location

Kerala Earthquake – 26-07-1953.
Epicentre: 9.9 N, 76.3 E.
Magnitude: ~ 5.1.
Depth of focus: NA (Avg. depth of 15 km is assumed).

Lat.	Long.	Intensity EMS 98	ED, km	PGA (g)
10.01	76.22	4	15	0.037
9.57	76.98	3	83	0.007
8.5	76.95	3	171	0.004
9.91	78.12	3	199	0.004
8.72	77.69	4	201	0.011

Lat. and Long. are the coordinates of the Intensity location
ED stands for Epicentral distance
PGA stands for Peak Ground Acceleration at the location

Bangalore Earthquake – 29-01–2001.
Epicentre: 12.595 N, 77.22 E.
Magnitude: ~ 4.2.
Depth of focus: ~ 15 km.

Lat.	Long.	Intensity EMS 98	ED, km	PGA (g)
12.71	77.27	2	14	0.006
12.58	77.04	3	20	0.013
12.54	77.42	5	23	0.084
12.67	77.46	5	27	0.077
12.38	77.05	3	30	0.011
12.52	76.89	3	37	0.010
12.2	77.03	2	49	0.003
12.96	77.58	5	56	0.055
13.1	77.38	3	59	0.008
12.41	76.69	3	61	0.008
12.3	76.65	3	70	0.007
11.92	76.94	3	81	0.007
13.07	77.79	3	81	0.007
13.34	77.1	2	84	0.003
12.99	77.93	4	89	0.017
13.14	78.14	2	117	0.002
12.87	74.84	2	260	0.001

Lat. and Long. are the coordinates of the Intensity location
ED stands for Epicentral distance
PGA stands for Peak Ground Acceleration at the location

Bangalore Earthquake – 20-03-1984.
Epicentre: 12.55 N, 77.77 E.
Magnitude: ~ 4.7.
Depth of focus: NA (Avg. depth of 15 km is assumed).

Lat.	Long.	Intensity EMS 98	ED, km	PGA (g)
12.56	77.75	5	2	0.115
12.53	77.78	5	2	0.115
12.58	77.8	6	5	0.293
12.6	77.88	5	13	0.099
12.62	77.92	4	18	0.035
12.7	77.69	5	19	0.089

12.73	77.82	5	21	0.086
12.82	77.78	5	30	0.074
12.8	77.6	5	33	0.071
12.97	77.59	5	51	0.058
13.29	77.53	4	86	0.017
12.31	76.64	3	126	0.005

Lat. and Long. are the coordinates of the Intensity location
ED stands for Epicentral distance
PGA stands for Peak Ground Acceleration at the location

Mysore Earthquake – 12-02-1970.
Epicentre: 13 N, 76.1 E.
Magnitude: ~ 5.2.
Depth of focus: NA (Avg. depth of 15 km is assumed).

Lat.	Long.	Intensity EMS 98	ED, km	PGA (g)
12.78	76.23	4	28	0.029
12.67	76.27	3	41	0.010
12.63	76.05	3	41	0.009
12.3	76.29	4	81	0.017
13.31	76.93	3	96	0.006
12.3	76.65	4	98	0.016

Lat. and Long. are the coordinates of the Intensity location
ED stands for Epicentral distance
PGA stands for Peak Ground Acceleration at the location

References

Anbazhagan, P., 2013. Method for seismic microzonation with geotechnical aspects. Disaster Adv. 6 (4), 66–86.
Anbazhagan, P., Smitha, C., Kumar, A., 2014. Representative seismic hazard map of Coimbatore, India. Eng. Geol. 171, 81–95.
Anbazhagan, P., Bajaj, K., Moustafa, S.S.R., Al-Arifi, N.S.N., 2015. Maximum magnitude estimation considering the regional rupture character. J. Seismol. 19 (3), 695–719.
Atkinson, G.M., Boore, D.M., 2006. Earthquake ground-motion prediction equations for Eastern North America. Bull. Seismol. Soc. Am. 96 (6), 2181–2205.
Atkinson, G.M., Boore, D.M., 2011. Modifications to existing ground-motion prediction equations in light of new data. Bull. Seismol. Soc. Am. 101 (3), 1121–1135.
Azarbakht, A., Rahpeyma, S., Mousavi, M., 2014. A new methodology for assessment of the stability of ground-motion prediction equations. Bull. Seismol. Soc. Am. 104 (3), 1447–1457.
Bajaj, K., Anbazhagan, P., 2019. Regional stochastic ground-motion model for low to moderate seismicity area with variable seismotectonic: application to Peninsular India. Bull. Earthq. Eng. 17 (7), 3661–3680.
Balakrishnan, T.S., Unnikrishnan, P., Murty, A.V.S., 2009. The tectonic map of India and contiguous areas. J. Geol. Soc. India 74 (2), 158–168.
Basu L., K., 1964. A note on the Coimbatore earthquake of 8th February 1900. Indian Journal of Meteorology and Geophysics 15 (2), 281–286.
Boore, D.M., Atkinson, G.M., 2008. Ground-motion prediction equations for the average horizontal component of PGA, PGV, and 5%-Damped PSA at spectral periods between 0.01 s and 10.0 s. Earthquake Spectra 24 (1), 99–138.
Boore, D.M., Joyner, W.B., 1997. Site amplifications for generic rock sites. Bull. Seismol. Soc. Am. 87 (2), 327–341.
Budnitz, R.J., Apostolakis, G., Boore, D.M., Cluff, L.S., Coppersmith, K.J., Cornell, C.A., Morris, P.A., 1997. Recommendations for probabilistic seismic hazard analysis—guidance on uncertainty and use of experts. In: Washington, D. C., U.S. Nuclear Regulatory Commission NUREG/CR–6372, 1.
Campbell, K.W., 2003. Prediction of strong ground motion using the hybrid empirical method and its use in the development of ground-motion (attenuation) relations in Eastern North America. Bull. Seismol. Soc. Am. 93 (3), 1012–1033.
Delavaud, E., Scherbaum, F., Kuehn, N., Allen, T., 2012. Testing the global applicability of ground-motion prediction equations for active shallow crustal regions. Bull. Seismol. Soc. Am. 102 (2), 707–721.
FEMA, 2005. Federal Guidelines for Dam Safety-Earthquake Analyses and Design of Dams. Federal Emergency Management Agency.
Ganesha Raj, K., Nijagunappa, R., 2004. Major Lineaments of Karnataka State and their relation to seismicity: a remote sensing based analysis. J. Geol. Soc. India 63 (4), 430–439.
Gupta, I., 2006. Delineation of probable seismic sources in India and neighbourhood by a comprehensive analysis of seismotectonic characteristics of the region. Soil Dyn. Earthq. Eng. 26 (8), 766–790.
Heaton W., T., Tajima, F., Mori W., A., 1986. Estimating ground motions using recorded accelerograms. Surv. Geophys. 8 (1), 25–83.
Hwang, H., Huo, J.-R., 1997. Attenuation relations of ground motion for rock and soil sites in eastern United States. Soil Dyn. Earthq. Eng. 16 (6), 363–372.
ICOLD, 2009. Selecting Seismic Parameters for Large Dams. Guidelines. ICOLD.
IS 1893 (Part 1), 2016. Criteria for Earthquake Resistant Design of Structures-Part 1 General Provisions and Buildings. Bureau of Indian Standards.
Iyengar, R.N., Raghu Kanth, S.T.G., 2004. Attenuation of strong ground motion in Peninsular India. Seismol. Res. Lett. 75 (4), 530–540.
Jaiswal, K., Sinha, R., 2007. Probabilistic seismic-hazard estimation for Peninsular India. Bull. Seismol. Soc. Am. 97 (1B), 318–330.
Kayal, J.R., 2008. Microearthquake Seismology and Seismotectonics of South Asia. Springer, Netherlands.
Kijko, A., Singh, M., 2011. Statistical tools for maximum possible earthquake magnitude estimation. Acta Geophysica 59 (4), 674–700.
Gardner, J.K., Knopoff, L., 1974. Is the sequence of earthquakes in southern California, with aftershocks removed, Poissonian? Bull. Seismol. Soc. Am. 64 (5).
Krinitzsky, E.L., 1995. Deterministic versus probabilistic seismic hazard analysis for critical structures. Eng. Geol. 40 (1–2), 1–7.
Martin, S., Szeliga, W., 2010. A catalog of felt intensity data for 570 Earthquakes in India from 1636 to 2009. Bull. Seismol. Soc. Am. 100 (2), 562–569.
Nath, S.K., Thingbaijam, K.K.S., 2011. Peak ground motion predictions in India: an appraisal for rock sites. J. Seismol. 15 (2), 295–315.
Nath, S.K., Mandal, S., Adhikari, M.D., Maiti, S.K., 2017. A unified earthquake catalogue for South Asia covering the period 1900–2014. Nat. Hazards 85 (3), 1787–1810.
NDMA, 2010. Development of probabilistic seismic hazard map of India. In: Technical Report by National Disaster Management Authority. Government of India.
Nuss, L.K., Matsumoto, N., Hansen, K.D., 2012. Shaken, but not stirred: earthquake performance of concrete dams, innovative dam and levee design and construction for sustainable water management. In: Proc., 32nd Annual USSD Conf., New Orleans, pp. 1511–1530.
Oldham, R.D., 1883. A catalogue of Indian earthquakes from the earliest time to the end of A.D. 1869. Mem. Geol. Surv. India 19 (3), 163–215.
Pailoplee, S., 2014. Earthquake hazard of dams along the Mekong mainstream. Nat. Hazards 74 (3), 1813–1827.
Parvez, I.A., Magrin, A., Vaccari, F., Ashish, C., Mir, R.R., Peresan, A., Panza, G.F., 2017. Neo-deterministic seismic hazard scenarios for India—a preventive tool for disaster mitigation. J. Seismol. 21 (6), 1559–1575.
Pezeshk, S., Zandieh, A., Tavakoli, B., 2011. Hybrid empirical ground-motion prediction equations for Eastern North America using NGA models and updated seismological parameters. Bull. Seismol. Soc. Am. 101 (4), 1859–1870.
Ramasamy, S.M., 2006. Remote sensing and active tectonics of South India. Int. J. Remote Sens. 27 (20), 4397–4431.
Rao, B., 2000. Historical seismicity and deformation rates in the Indian Peninsular Shield. J. Seismol. 4 (3), 247–258.
Rao, B., 2015. Seismic Activity - Indian Scenario. Buddha Publisher, Hyderabad, India.
Reiter, L., 1990. Earthquake Hazard Analysis: Issues and Insights. Columbia University Press, New York.
Scherbaum, F., Delavaud, E., Riggelsen, C., 2009. Model selection in seismic hazard analysis: an information-theoretic perspective. Bull. Seismol. Soc. Am. 99 (6), 3234–3247.
SEISAT, 2000. Seismotectonic Atlas of India and its Environs. Geological Survey of India, India.
Seyrek, E., Tosun, H., 2011. Deterministic approach to the seismic hazard of dam sites in

Kızılırmak basin, Turkey. Nat. Hazards 59 (2), 787–800.
Sitharam, T.G., Anbazhagan, P., 2007. Seismic hazard analysis for the Bangalore region. Nat. Hazards 40 (2), 261–278.
Sitharam, T.G., James, N., Vipin, K.S., Ganehsa Raj, K., 2012. A study on seismicity and seismic hazard for Karnataka State. J. Earth Syst. Sci. 121 (2), 475–490.
Sitharam, T.G., Kolathayar, S., James, N., 2015. Probabilistic assessment of surface level seismic hazard in India using topographic gradient as a proxy for site condition. Geosci. Front. 6 (6), 847–859.
Tavakoli, B., Pezeshk, S., 2005. Empirical-stochastic ground-motion prediction for Eastern North America. Bull. Seismol. Soc. Am. 95 (6), 2283–2296.
Toro, G.R., Abrahamson, N.A., Schneider, J.F., 1997. Model of strong ground motions from earthquakes in Central and Eastern North America: best estimates and uncertainties. Seismol. Res. Lett. 68 (1), 41–57.
Vetter, U.R., Ake, J.P., Laforge, R.C., 1997. Seismic hazard evaluation for dams in northern Colorado, U.S.A. Nat. Hazards 14 (2–3), 227–240.
Vipin, K.S., Anbazhagan, P., Sitharam, T.G., 2009. Estimation of peak ground acceleration and spectral acceleration for South India with local site effects: probabilistic approach. Nat. Hazards Earth Syst. Sci. 9 (3), 865–878.
Vita-finzi, C., 2004. Buckle-controlled seismogenic faulting in peninsular India. Quat. Sci. Rev. 23 (23–24), 2405–2412.
Wells, D.L., Coppersmith, K.J., 1994. New empirical relationships among magnitude, rupture length, rupture width, rupture area, and surface displacement. Bull. Seismol. Soc. Am. 4 (84), 975–1002.
Wheeler, R.L., 2009. Methods of Mmax estimation east of the rocky mountains. In: USGS Report.
Wiemer, S., Wyss, M., 2000. Minimum magnitude of completeness in Earthquake Catalogs: Examples from Alaska, the Western United States, and Japan. Bull. Seismol. Soc. Am. 90 (4), 859–869.